SUPRAMOLECULAR ANTIMICROBIAL CAPSULES ASSEMBLED FROM POLYOXOMETALATES AND CHITOSAN

Laura De Matteis, Scott G. Mitchell and Jesús M. de la Fuente

One of the principle advantages offered by nanohybrid materials is the possibility to construct modular composite assemblies derived from varied and responsive components and whose properties are superior to those of the single components. Polyoxometalates (POMs for short) are a prominent and diverse class of nanoscale molecular metal-oxides characterized by a broad and versatile range of physicochemical properties. Their redox behaviour in particular lends them to a wide variety of applications including catalysis and medicine. Due to their high electronic charge, POMs display a particular affinity towards biomolecules. The behaviour and dynamics of POMs can be enhanced significantly by the use of inexpensive carriers and supports that possesses mechanical stability, regenerability and reactive functional groups. For most bioapplications, the use of polymeric nanoscaffolds and nanocarriers are convenient for a number of factors, including controlled drug delivery and release as well as improving interactions with cells. Chitosan is a biocompatible and biodegradable polysaccharide obtained from chitin deacetylation. The presence of free amino and hydroxyl groups makes chitosan a cationic polyelectrolyte with chelating and bioadhesive properties. Consequently, this cheap and abundant linear polysaccharide is capable of interacting with POMs to produce hybrid organic–inorganic multilayer films, networks and capsules. Several POMs, specially the polyoxomolybdates, have recognised antibacterial activity, against both Gram-negative and Gram-positive bacteria. However in spite of the promising biotechnological applications of POM-chitosan materials, the antibacterial activity of such hybrid materials has only recently been described and, to the best of our knowledge, the structural relation between POM-chitosan composites and their antibacterial activity has never been comprehensively investigated. This communication reports the synthesis, characterization and antibacterial activity of a series of nanometre-sized capsules obtained through the supramolecular assembling of polyoxometalates, chitosan and cetyltrimethylammonium bromide (CTAB). Using a micelle-based approach, the surfactant is used as a cationic nucleating agent as well as a tool to trap the POMs before being enveloped by the structure-directing chitosan polymer matrix (Fig. 1a). The antibacterial activity of these nanoscale composite capsules was evaluated against E.coli. The three representative POMs chosen for this study were H3PW12O40 (phosphotungstic acid, PTA), H3PMo12O40 (phosphomolybdic acid, PMA) and (NH4)15{Na[(Mo2O4)6(μ2-SO3)3-(μ2-SO3)]2}.5H2O (Kabanos). The preparation of the capsules followed analogous procedures where only the POM was altered. The first fundamental step consisted in the drop wise addition under sonication of 0.2 M CTAB in EtOH (96%) to an aqueous solution of the desired POM (PTA, PMA or Kabanos), which resulted in the formation of POM-decorated micelles (the micelle-core of the final capsule). After that an equivalent volume of 5 mg mL_1 chitosan solution was added under a short sonication (2 min) producing the intimate mix of the polymer with POM-decorated micelles. Finally, complex coacervation of the suspension of capsules was carried out by adding them to a solution of 50 mM Na2SO4 (aq) under ultrasonication.

The resulting hybrid capsules were washed and resuspended in ddH2O. A detailed description of the experimental procedure is reported in ESI. As the POMs selected for this study each possess distinctive colours (PTA ¼ white, PMA ¼ green and Kabanos ¼ orange), their incorporation into the polymer matrix could be verified by eye in the first instance since the colours of the colloidal suspensions were commensurate with the corresponding POMs employed in the synthesis (Fig. S1).
The structure of the capsules and their final composition were investigated in detail by means of Scanning and Transmission Electron Microscopy techniques, SEM (field emission SEM Inspect F50 (FEI) with an EDX system INCA PentaFETx3 in an energy range between 0–30 keV) and BF-TEM (FEI Tecnai F30 operating at 300 keV), as well as by Fourier Transform Infrared Spectroscopy (FTIR). The regular morphology and size of the composites is shown in (Fig. 1b–e and S2–S4). The capsules synthesised using polyoxomolybdates (Kabanos and PMA) were found to possess diameters in the range of 100–200 nm, whereas the polyoxotungstate capsules (PTA) were somewhat larger in the range of 200–300 nm (Fig. S7–S9). The presence of polymeric chitosan and CTAB as major part of these composite capsules materials meant that obtaining suitable electron microscopy images was complicated due to the high vacuum and voltages required by these techniques, which were found to deform and burn the samples, respectively. Nevertheless, highresolution SEM images were obtained (Fig. 1b–d) and embedding the capsules in a gelatin resin assisted with this task (Fig. 1e and S5). Further, BF-TEM data goes one step closer to revealing the morphology and composition of the capsules and Fig. 1f clearly illustrates how a higher contrast area can be observed corresponding to the hybrid polymer–metal shell of the capsule. Energy-Dispersive X-ray spectroscopy (EDX) spectra of the capsules confirmed the presence of metals Mo and W from the POMs (See Fig. S10–S12).
FTIR spectroscopy was used to further verify and compare the composition of the metal–organic hybrid capsules with the corresponding starting materials. These data show that the most prominent stretching and vibration regions of all starting materials can be identified in the composite materials. Fig. 2 provides a representative example of the components and corresponding capsule formed using the Kabanos POM. The POM encapsulated within this particular capsule showed characteristic stretches at 1637 (H2O), 1408 (NH4+), 1088 (SO3 2_), 981 and 963 (Mo-O), 865 and 809 cm_1 (SO3 2_). The Mo-O stretching frequencies at 981 and 963 were identified in the capsules spectrum and showed no significant shifts with respect to the precursors indicating the incorporation of the intact POM into the polymer hybrid capsules. Notably, due to the cationic exchange of the ammonium cation with CTAB during capsule formation, the characteristic ammonium stretch at 1408 cm_1 is absent in the Kabanos capsule spectrum, thus indicating a complete cationic exchange. Free CTAB on the other hand shows two further strong stretches at 2920 and 2850 cm_1 corresponding to (–CH2) as well as one at 2949 (N–CH3) that is enhanced in the case of CTAB packing. All of these were identified in the capsules, in addition to 912 and 961 (C–N), 1470 (RN(CH3)3 +), 720 and 728. The Kabanos capsule spectrum also displayed clear evidence of chitosan, namely at 1645 (primary amide), 1414 (–CH2), 1375 (–CH3) and 1150 cm_1 (C–O–C skeletal vibrations).

A peak at 1530 cm_1 appears only in the capsule spectrum, probably indicating the protonated amino group from chitosan (pure chitosan was measured as a powder, therefore with the amino group unprotonated). The FTIR spectra of capsules containing PMA and PTA show similar effects (Fig. S13–S15/Table S1). Since POMs display antibacterial activity toward both Gramnegative and Gram-positive bacteria, the antimicrobial activities of our hybrid capsules were tested against E.coli and compared with that of the corresponding POMs in aqueous solution (free POMs) to investigate how POM encapsulation affected their antibacterial activity. None of the free POMs showed any antibacterial activity up to a concentration of 0.5 mg mL_1 after 7 h incubation with E.coli. Resazurin viability assays of E.coli after 7 h incubation with Kabanos, PMA and PTA are reported in ESI together with bacteria growth curves reporting optical density variation of E.coli suspension depending on capsule concentration. Fig. S17 shows graphs of the antibacterial growth inhibition assays of POM-based capsules. All control experiments and antibacterial assays were repeated a total of six times to verify the reproducibility of the results and to calculate the mean values and associated standard deviation errors that are shown on the graphed results of these assays. An outstanding difference between the antimicrobial activity of the composite capsules and 'free' POMs was observed in the case of polyoxomolybdates PMA and Kabanos. While the free polyoxomolybdates showed no antimicrobial activity up to a concentration of 0.5 mg mL_1, hybrid materials based on the corresponding POMs presented a significant antibacterial effect; especially those containing PMA, which produced a decrease of 80% viability even at a capsule concentration of as little as 50 μgmL_1. No antibacterial activity was observed for either the free polyoxotungstate (PTA) or the PTA-based capsules at tested concentrations (Fig. S17). Although antibacterial assays showed potent antibacterial activity of polyoxomolybdate-based capsules (Kabanos and PMA) compared with inactivity of the polyoxotungstate variant (PTA), Environmental Scanning Transmission Electron Microscopy (ESTEM) images of E.coli incubated with these capsules provide additional insight. ESTEM imaging demonstrated how each capsule variant clearly elicits distinct responses from the bacterium cell, indicative of different particle–bacterium interactions (Fig. 3). Bacterial cells incubated with Kabanos and PMA capsules show evidence of stress and damage (Fig. S19 and S20); while those incubated with PTA appear unaltered (Fig. S21). In order to help illustrate the potent antibacterial activity of the polyoxomolybdate nanocapsules compared with the polyoxotungstate nanocapsules, Fig. 3 includes a graph of the %E.coli cell death observed after 7 h incubation with 0.5 mg mL_1 of 'free' POMs compared with their corresponding nanocapsules at the same concentration. In the case of PMA-containing capsules the reported antimicrobial effect can be associated with a direct interaction between the bacterium cell and capsules, which seem to be massively internalised (Fig. 3b and S20). Interestingly in the case of the Kabanos-based capsules, a direct interaction between composite material and bacteria surface could not be clearly recognized from the ESTEM images; yet the cell surface appeared dramatically damaged after incubation with capsules, clearly indicating signs of stress (Fig. 3a and S19).

Based on recent antibacterial studies on POM-chitosan aggregates, the increased antibacterial activity of the capsules presented in this communication could be attributed to both their shape and size. Although all of the capsules are undoubtedly polydisperse, a comparison between the size distribution of the molybdatebased capsules (PMA and Kabanos) reveal diameters in the size range of 100–200 nm (Fig. S7 and S8) while the tungstate-based capsules fall in the range of 200–300 nm (Fig. S9). Consequently, the potent antibacterial activity of the molybdate-based capsules could be due to their spherical shape combined with their tendency to form more disperse capsules of smaller size. Detailed studies are now underway to further investigate and determine more precisely the exact mechanisms responsible for the antibacterial action of these composite materials.

CONCLUSIONS

Composite capsules based on metal–polymer suparamolecular architectures have been designed to incorporate different polyoxometalates (PMA, Kabanos and PTA). Comprehensive characterization of these materials indicate a metal–organic hybrid structure based on POM-decorated micellar CTAB cores interwoven with chitosan-coordinated POMs. Finally their antimicrobial properties were tested against a non-pathogenic Escherichia coli strain. While capsules based on polyoxomolybdate ariants showed potent antibacterial activity, polyoxotungstate capsules showed no antimicrobial effect. Subsequent electron microscopy studies of the capsules and the bacteria provide the first lines of evidence that the each polyoxomolybdate-capsule variant elicits distinct responses from the bacteria, indicative of different particle–bacterium interactions. Detailed mechanistic studies are currently underway.

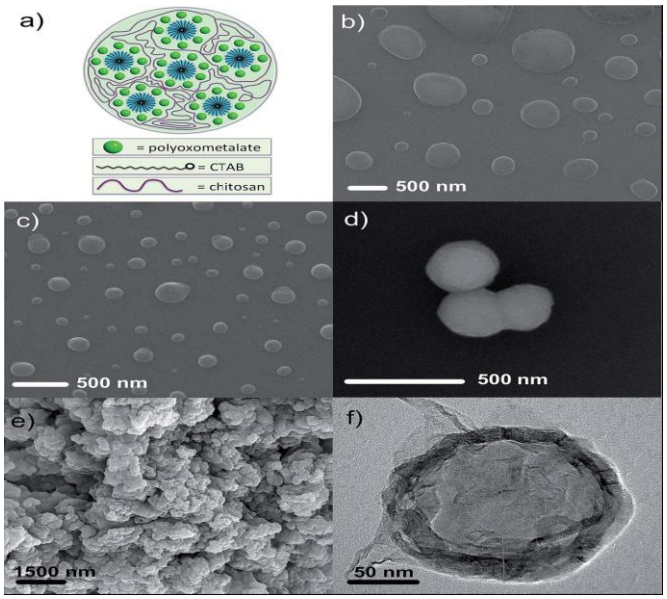

Fig. 1 (a) Overview of hybrid capsule composition. SEM images of composite capsules based on (b) Kabanos; (c) PMA; and (d) PTA. (e) SEM image of Kabanos capsules bound in gelatine; and (f) BF-TEM of a discrete Kabanos capsule embedded in gelatine.

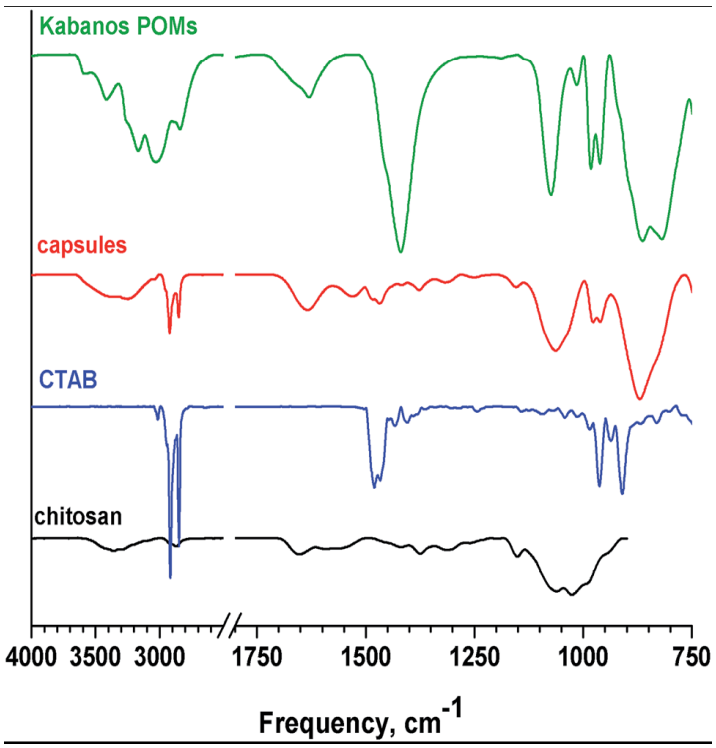

Fig. 2 FTIR spectra of Kabanos-based capsules in comparison with their component parts: single crystals of the Kabanos POM, CTAB and liquid chitosan (refer to Fig. S13–S15 and Table S1† for further details).

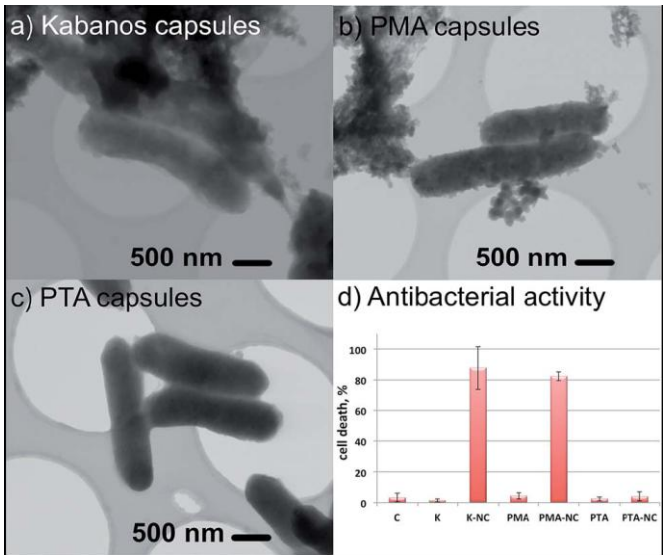

Fig. 3 Environmental STEM images of E.coli incubated with (a) Kabanos-; (b) PMA-; and (c) PTA-based chitosan capsules, fixed with glutaraldehyde, washed three times and resuspended in water. (d) Antibacterial activity of 0.5 mg mL_1 of control (C), 'free' Kabanos (K), PMA and PTA compared with their corresponding nanocapsules (NC) at the same concentration. Note that antibacterial assays were repeated six times to calculate mean values and associated standard deviations and also that nanocapsules may appear somewhat aggregated in the ESTEM images as a result of the bacterial fixation protocol with glutaraldehyde.